Hue University Journal of Science: Natural Science
Vol. 131, No. 1D, 23–36, 2022

pISSN 1859-1388
eISSN 2615-9678

Simple thermal-electrical model of photovoltaic panels with cooler-integrated sun tracker

Ngo Xuan Cuong[1*], Huynh Thi Thuy Linh[1], Nguyen Dinh Hoa Cuong[1], Nguyen Duy Thuan[1], Le Vinh Thang[2, 3], Nguyen Thi Hong[4]

[1] School of Engineering and Technology, Hue University, 1 Dien Bien Phu St., Hue, Vietnam
[2] Hue University, Quang Tri Branch, Dien Bien Phu St., Quang Tri, Vietnam
[3] Department of automatic control system and control, National Research University of Electronic Technology (MIET), ld. 1, Shokin Square, Zelenograd, Moscow, Russia
[4] Hue Industrial College, 70 Nguyen Hue St., Hue, Vietnam

* Correspondence to Ngo Xuan Cuong <ngoxuancuong@hueuni.edu.vn>

(*Received: 12 April 2022; Accepted: 20 June 2022*)

Abstract. This paper presents a simple thermal-electrical model of a photovoltaic panel with a cooler-integrated sun tracker. Based on the model and obtained weather data, we analyzed the improved overall efficiency in a year as well as the performance in each typical weather case for photovoltaic panels with fixed-tilt systems with a tilt angle equal to latitude, fixed-tilt systems with cooler, a single-axis sun tracker, and a cooler-integrated single-axis sun tracker. The results show that on a sunny summer day with few clouds, the performance of the photovoltaic panels with the proposed system improved and reached 32.76% compared with the fixed-tilt systems. On a sunny day with clouds in the wet, rainy season, because of the low air temperature and the high wind speed, the photovoltaic panel temperature was lower than the cooler's initial set temperature; the performance of the photovoltaic panel with the proposed system improved by 12.55% compared with the fixed-tilt system. Simulation results show that, over one year, the overall efficiency of the proposed system markedly improved by 16.35, 13.03, and 3.68% compared with the photovoltaic panel with the fixed-tilt system, the cooler, and the single-axis sun tracker, respectively. The simulation results can serve as a premise for future experimental models.

Keywords: thermal-electrical model, sun tracker, photovoltaic, cooling system, efficiency, fixed-tilt system

1 Introduction

Currently, numerous government decisions and action programs have contributed to promoting the development of solar power systems in Vietnam. The advantage of solar photovoltaic (PV) systems is that they create no pollution during operation and, at the same time, reduce global warming and operating and maintenance costs compared with other solar technologies. However, PV technology, in general, and grid-tied solar power, in particular, have some common problems that need to be solved, including low efficiency and being negatively affected by hail, dust, and surface temperatures. The performance of PV panels is mainly affected by the temperature and direction of solar radiation relative to the work surface. Therefore, building a research model to improve the efficiency of the PV system is crucial. In addition, improving the efficiency of the system also contributes to increasing grid-connected electricity output, shortening the investment payback period of solar power projects, saving

system installation space, and using energy economically and efficiently.

An experimental evaluation of a water-film cooling system for commercial photovoltaic panels was conducted at the Polytechnic School, University of São Paulo, São Paulo, Brazil [2]. The results show that the cooling system reduced the temperature by 15–19% on average, with a maximum of 35%. Regarding power, there was an average augmentation of 5–9% with a maximum augmentation of 12%. The total yield increased by 2.3–6% on average, with a maximum of 12% [2].

In 2017, an experimental study on the effect of cooling a panel with air and water was carried out in Coimbatore, India [8]. The results reveal that the temperature of the PV panels ranged from 31 to 62 °C without cooling. Meanwhile, it changed from 30 to 43 °C and from 30.6 to 37.8 °C with air cooling and water cooling. The power output of the PV panels during a study day without cooling, with air cooling for the upper surface, with air cooling for the bottom surface, with water cooling for the upper surface, and with water cooling for the bottom surface is 3.1, 3.4, 3.6, 3.9, and 4.2 kWh, respectively. Thus, the efficiency improvement of the PV panels with a water cooling system was 25.8–35.48% compared with those without cooling.

A study on the front, back, and both-surface active water cooling for the photovoltaic panels was conducted for a 50 W photovoltaic panel with an inclination angle of 17° in a Mediterranean climate (the City of Split is located on the Croatian coast) [11]. The results show that the electrical efficiency increased linearly with increasing the flow of water sprayed on the surface of the photovoltaic panel. The average temperature of the panels decreased from 52 to 24 °C, and the lowest temperature was limited by the water temperature in the pipeline, which remained constant at 17 °C. The improved efficiency of the PV panels with front surface spray, back surface spray, and both surface sprays was 14.6, 14.0, and 16.3%, respectively, compared with PV panels without spray.

A study on the effect of water cooling on single and polycrystalline PV panels was conducted on August 6, 2020, in Tehran [14]. The PV panels were installed at a south angle and an angle of inclination equal to the latitude of the study site. The cooling water was allowed to flow directly onto the surface of the PV panels to form a water film. Using mathematical modelling and experimentation on a hot summer day, the researchers found that the optimum water flow rate was around 0.01 kg/s with a power improvement efficiency of 3.84 and 4.20% for cooled polycrystalline and monocrystalline PV panels compared with uncooled PV panels. The results also show that the wind speed affected the PV panel power output, but its increase in rate was much lower than that of water cooling.

Research on improving performance with sun trackers has also been conducted by numerous researchers. A study on a single-axis sun tracker for a 250Wp PV panel in central Vietnam indicated that maximum overall energy improvement increased by 30.3% on a sunny day upon using the proposed tracking system [10]. Furthermore, the net energy obtained by using the sun tracker was 15.2% under typical weather conditions. In addition, the sun tracker consumed about 2–8% of the system's power output.

An experimental study on the effect of cooling with phase-change materials on a sun tracker integrated with a concentrated photovoltaic thermal system was conducted at the University of Macau campus on Hengqin island [17]. The results show that the proposed system increased the electrical, thermal and overall efficiency by more than 10, 5, and 15%,

pISSN 1859-1388
eISSN 2615-9678

respectively, compared with a similar water-cooling system.

At the Harbin Institute of Technology at Weihai, a photovoltaic-thermal system with a sun tracker integrated with a cooling SiO_2/TiO_2 thin film was studied [5]. Outdoor testing shows that the PV panels with the proposed system could reduce three degrees, improve power generation efficiency by 10%, and increase the overall energy by 4.94% [5].

Cooling PV panels allows one to increase photovoltaic conversion efficiency as well as capture waste heat, which can be used for different purposes [12]. Research at the laboratory of the Department of Energy at the Cracow University of Technology shows that aluminum radiators and a water-glycol cooling mixture helped increase the power output of PV panels with a sun tracker by about 4–6% on sunny days. The power output of PV panels with the sun tracker increased from 32 to 65%, compared with fixed inclined PV panels [12].

The analysis above indicates that the performance of PV panels can be improved by using sun trackers and water coolers. However, there are few studies on combined systems with a need for long-term analysis results. Therefore, in this study, we focus on two aspects. First, we developed a simple thermal-electrical model for PV panels with a cooler-integrated sun tracker. Second, we compared the overall efficiency of the proposed PV panel with the fixed-tilt system, the water cooler, and the single-axis sun tracker over one year via simulation.

The rest of the paper is arranged as follows: Section 2 introduces research methods and system description. Section 3 presents a model of PV panels with a cooler-integrated single-axis sun tracker. In Section 4, a comparative investigation of the proposed system, a fixed-tilt system, a fixed-tilt system with a cooler, and a single-axis sun tracker was conducted with simulation results. Our conclusions were drawn in the final section.

2 Methods and system description

2.1 Methods

The following methods were used to conduct the research.

Modelling: Under certain assumptions, the PV panels with a cooler-integrated single-axis sun tracker were described in a simple thermal-electrical model.

Data synthesis: The Solcast 2020 weather data were selected as global horizontal irradiance (*GHI*), direct normal irradiance (*DNI*), diffuse horizontal irradiance (*DHI*), air temperature, and wind speed [16].

Data analysis: The PV panel system simulation data for one year were analyzed and compared among four systems: fixed-tilt panels with tilt angle equal to latitude, fixed-tilt panels with a cooler, single-axis panels with a sun tracker, and cooler-integrated single-axis panels with a sun tracker.

2.2 System description

The object of the study is a PV panel with a cooler-integrated single-axis sun tracker (Fig. 1). The study site is Hue City, central Vietnam, with a latitude of 16.45°N and a longitude of 107.6°E.

The polycrystalline photovoltaic panels SUN330-72P were selected in this study with the specifications shown in Table 1.

There are four offered independent models, including a model with a sun tracker, a model with a water spray cooler, a PV panel thermal model, and a PV panel electrical model. We studied all the models in terms of their

temperature and the solar radiation shining on their surfaces.

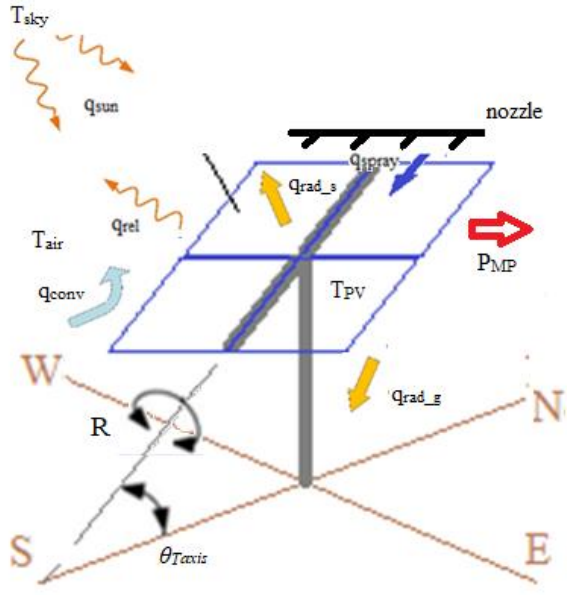

Fig. 1. PV panel with cooler-integrated sun tracker

Table 1. Characteristics of PV panel under standard test conditions

PV panel	Specifications
Type of cells	Polycrystalline
Power rating	330 Wp
Panel efficiency	17.09%
Number of cells	72
Voltage at maximum power	37.8 V
Current at maximum power	8.73 A
Short circuit current	9.22 A
Open circuit voltage	45.5 V
Temperature coefficient of P_{max}	−0.41%/°C
Temperature coefficient of V_{oc}	−0.33%/°C
Temperature coefficient of I_{sc}	0.06%/°C
Panel dimension	1950 × 990 × 40 mm
Weights	23 kg
Lifetime	21–25 years

3 Model of PV panels with cooler-integrated single-axis sun tracker

3.1 Model of sun tracker

Solar radiation on inclined plane

The total solar irradiance on an inclined surface can be calculated according to Eq. 1 [9].

$$G_t = G_b + G_g + G_d \quad (1)$$

where G_b is the beam irradiance; G_g is the ground-reflected irradiance; G_d is the sky-diffuse irradiance.

Sky-diffuse irradiance can be calculated based on Liu and Jordan's model according to Eq. 2.

$$G_d = DHI\,\frac{1+\cos\theta_T}{2} \quad (2)$$

where *DHI* is the diffuse horizontal irradiance, W/m²; θ_T is the tilt angle of the PV panel surface, degree.

Ground-reflected irradiance can be calculated according to Eq. 3.

$$G_g = GHI.\text{albedo}.\frac{1-\cos\theta_T}{2} \quad (3)$$

where *GHI* is the global horizontal irradiance, W/m²; *albedo* is the ground albedo (usually equal to 0.2).

Beam irradiance can be calculated according to Eq. 4.

$$G_b = DNI \times \cos(AOI) \quad (4)$$

where *DNI* is the direct normal irradiance, W/m²; *AOI* is the angle of incidence, degree. The *AOI* is the angle between the ray of sunlight and the normal to the surface of the PV panel (Fig. 2), and it can be calculated according to Eq. 5 [7].

$$\cos(AOI) = \cos(\theta_z)\times\cos(\theta_T) + \sin(\theta_z)\times \sin(\theta_T)\times\cos(\gamma_s - \theta_A) \quad (5)$$

where θ_T is the tilt angle of the PV panel surface, degree; θ_z is the solar zenith, degree; θ_A is the

pISSN 1859-1388
eISSN 2615-9678

azimuth angle of the PV panel surface, degree; γ_s is the solar azimuth, degree.

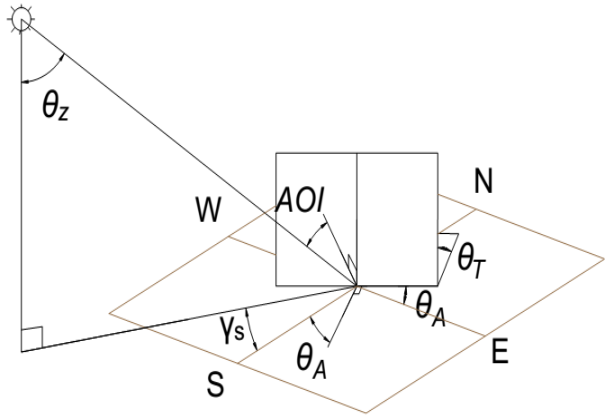

Fig. 2. Angle of incidence of PV panel

Solar declination may be estimated according to Eq. 6 [4]

$$\delta = 23.45 \times \sin(\frac{360(284+n)}{365}) \quad (6)$$

where n is the day number during a year, with January 1 being 1.

The hour angle and local solar time are calculated according to Eq. 7 [4]

$$\begin{gathered} \omega = 15 \times (LST - 12) \\ LST = ST + \frac{4 \times (L_{stm} - L_{loc}) + E}{60} \\ E = 9.87 \times \sin(2 \times B) - 7.53 \times \cos(B) - 1.5 \times \sin(B) \\ B = \frac{360 \times (n-81)}{365} \end{gathered} \quad (7)$$

where LST is the local solar time, h; ST is the standard time; E is the correction time, min; B is the variable for correction time, degree; L_{stm} is the longitude of the standard meridian for the local time zone; L_{loc} is the longitude of the studied area.

The position of the sun is determined with the solar azimuth angle, γ_s, and the solar zenith angle, θ_z. The zenith angle is the angle between the vertical (the zenith) and the incident sun ray, with a value between –90 and 90° in the case of a horizontal plane; the zenith angle is the angle of incidence. Solar azimuth is the angle of the sun rays measured in the horizontal plane from the true south with respect to the northern hemisphere; the direction west is indicated with a positive sign. It has a value between –180 and 180°. The solar azimuth and solar zenith angle are calculated according to Eq. 8.

$$\begin{gathered} \theta_z = \cos^{-1}(\sin\delta \times \sin\varphi + \cos\varphi \times \cos\delta \times \cos\omega) \\ \gamma_s' = \sin^{-1}\left(\frac{\cos\delta \times \sin\omega}{\sin\theta_z}\right) \\ \gamma_s = \begin{cases} \gamma_s' \text{ if } \cos\omega \geq \frac{\tan\delta}{\tan\varphi} \\ -180 + |\gamma_s'| \text{ if } \cos\omega < \frac{\tan\delta}{\tan\varphi} \text{ and } LST < 12 \\ 180 - |\gamma_s'| \text{ if } \cos\omega < \frac{\tan\delta}{\tan\varphi} \text{ and } LST > 12 \end{cases} \end{gathered} \quad (8)$$

where ω is the hour angle; φ is the latitude of the studied area, degree.

Single-axis sun tracker

The single-axis tracker is used to help PV panels always face the sun and receive the most significant amount of radiation (Fig. 1). The sun tracker's axis of rotation is designed with an axis-tilt angle $\theta_{T,axis}$ (17°), and its projection on the horizontal plane coincides with the north – south axis of the earth, and the azimuth angle of the axis of rotation $\theta_{A,axis}$ is 0°. The axis rotation R has a value in the range of $\pm R_{max}$, and the rotation is zero when the normal of the PV panels lies in the vertical plane containing the rotation axis. It has a negative value in the morning and a positive value in the afternoon. Their value depends on the design of the tracker. In this study, R_{max} was selected at 45°.

For an optimal tracker system, the control is conducted according to the time of day, and the value of the corresponding rotation angle R gives the smallest angle of incidence. This value can be calculated according to Eq. 11 [1, 7].

$$R = \tan^{-1}[X] + \psi \quad (9)$$

where

$$\begin{gathered} X = \frac{\sin\theta_z \times \sin(\gamma_s - \theta_{A,axis})}{\sin\theta_z \times \cos(\gamma_s - \theta_{A,axis}) \times \sin\theta_{T,axis} + \cos\theta_z \times \cos\theta_{T,axis}} \\ \psi = \begin{cases} 180 & \text{if } (X < 0) \text{ and } (\gamma_s - \theta_{A,axis}) > 0 \\ -180 & \text{if } (X > 0) \text{and } (\gamma_s - \theta_{A,axis}) < 0 \\ 0 & \text{other} \end{cases} \end{gathered} \quad (10)$$

The tilt angle of the PV panel surface with the solar tracker is expressed as

$$\theta_T = \cos^{-1}[\cos R \times \cos \theta_{T,axis}] \quad (11)$$

Consequently, the azimuth angles of PV panel surface are expressed as

$$\theta_A = \theta_{A,axis} + \sin^{-1} \times [\frac{\sin R}{\sin \theta_T}] \text{ when } \theta_T \neq 0 \quad (12)$$

The solar irradiance placed on the PV panel of the single-axis sun tracker model can be calculated by using the tilt angles and azimuth angles of the PV panel surface, as well as the *GHI*, *DHI*, and *DNI* data.

3.2 Photovoltaic panel thermal model

Assumption

Photovoltaic panels can be modelled as a single solid mass at a uniform temperature (T_{PV}).

The temperature of the ground at the site of installation is equal to the air temperature.

The photovoltaic panels absorb heat, lose heat as convection to the surrounding environment and radiation to the ground and the sky with sky temperature, T_{sky}, and generate electrical power, P_{mp}. Furthermore, the PV panels lose heat as a result of heat transfer between the mist stream and cooling water and evaporation during the cooling misting process. The equation for energy balance is as follows:

$$C_{PV} \times \frac{dT_{PV}}{dt} = G_t \times A_{PV} - q_{rel} - P_{MP} - q_{rad_s} - q_{rad\_g} - q_{conv} - q_{sp} \quad (13)$$

where C_{PV} is the equivalent thermal capacitance of the PV panel, J/K; T_{PV} is the PV panel temperature, °C; G_t is the solar irradiance on the PV panel surface, W/m²; q_{ref} is the reflected solar irradiance, W; P_{MP} is the electric power output of the PV panel, W; q_{conv} is the convective heat transfer between the PV panel surface and the air, W; q_{rad_s} is the radiation heat transfer between the PV panel and the sky, W; q_{rad_g} is the radiation heat transfer between the PV panel and the ground, W; q_{sp} is the convective heat transfer between the PV panel and water spray, W.

Reflected solar irradiance

Solar radiation hits the surface of the PV panels, partly transmits through the protective glass, and partly reflects back to the sky. The component reflecting back to the sky is calculated according to Eq. 14.

$$q_{rel} = (1 - \tau_g) \times A_{PV} \times G_t \quad (14)$$

where τ_g is the transmissivity of the PV panel protection glass; A_{PV} is the surface area of the PV panels, m².

The transmissivity of PV panel protection glass is not constant; it is a function of the angle of incidence of solar radiation on the PV panel. To simplify the model, we assume an annual mean for this parameter without too much loss of precision at 0.96 [2].

Thermal capacitance of PV panel

PV panels are considered a single block of solid material at a uniform temperature with thermal capacitance calculated according to Eq. 15.

$$C_{PV} = A_{PV} \times \sum_i \rho_i \times x_i \times c_{p\_i} \quad (15)$$

where ρ_i is the density of the ith layer of material, kg/m³; x_i is the thickness of the ith layer, mm; c_{p_i} specific heat capacity, kJ/kg/K; A_{PV} is the surface area of the PV panels, m².

Conventional PV panels have four layers with thermal parameters presented in Table 2 [8]. The thermal capacitance of the PV panels is 25,464 J/K. This data is close to 22,800 J/K in one study [13], which shows that an exact value of C_{PV} is not required because a 50% change in the value of C_{PV} does not significantly change the performance of the model.

pISSN 1859-1388
eISSN 2615-9678

Table 2. Thermal parameters of PV panel layers

	Glass	Cell	Tedlar	EVA
x, mm	4	0.5	1	0.5
c_p, kJ/kg/K	0.8	0.7	1.01	3.135
ρ, kg/m^3	2482	2328	1720	1720

Radiation heat

Radiant heat loss can be calculated by considering the emissivity and temperature of the emitter and receiver surfaces. For simple modelling purposes, the sky can be thought of as a black body with temperature T_{sky}; the ground where the PV panels are installed has a temperature considered to be the same as the plate temperature of the air. Therefore, the radiation heat transfer can be estimated by two components with the following expressions [8]

$$q_{rad\_s} = A_{PV} \times \sigma \times \varepsilon_{rad} \times \left[(T_{PV} + 273)^4 - (T_{sky} + 273)^4\right]$$
$$q_{rad\_g} = A_{PV} \times \sigma \times \varepsilon_{rad} \times [(T_{PV} + 273)^4 - (T_{air} + 273)^4)] \quad (16)$$

where q_{rad_s} is the radiation heat transfer between the PV panel and the sky, W; q_{rad_g} is the radiation heat transfer between the PV panel and the ground, W; ε_{rad} is the thermal emissivity of the PV panel (about 0.9); σ is the Stephan-Boltzmann constant 5.68 × 10^{-8} W/m^2/K^4; T_{PV} is the PV panel temperature, °C; T_{sky} is the sky temperature in °C and is estimated according to Eq. 17 [8]

$$T_{sky} = 0.0552 \times {T_{air}}^{1.5} \quad (17)$$

Convective heat transfer between PV panel surface and air

The convection heat exchange component is related to the heat transfer between the PV panel and the environment, mainly due to the forced convection under the effect of wind speed. This study considers a linear model between the wind speed and the convective heat transfer coefficient. The modelled convective heat exchange between the PV panels and air is described by Eq. 18 [14, 15].

$$q_{conv} = A_{PV} \times h_{conv} \times (T_{PV} - T_{air})$$
$$h_{conv} = 3 \times v_{wind} + 2.8 \quad (18)$$

where v_{wind} is the wind speed, m/s; h_{conv} is the convection heat transfer coefficient, W/m^2/K; T_{air} is the air temperature around the PV panel, °C.

3.3 Model of water spray cooler

The cooler in this study was designed with the nozzles positioned at the higher part of the PV panel width so that they do not cast shadows. It was supplied with the water cooled by the pump motor with the highest water flow rate, MF_w, m^3/s, and the spray stream was directed to the entire area of the PV panel. The cooling water temperature was constant at 25 °C. The cooler operated in an on/off mode with a preset temperature of 45 °C and a delay of 5 °C.

The spray cooling process took place as follows: Water was pumped through small nozzles into the air, forming droplets spreading the entire surface of the PV panel. The water droplets spread on the surface evaporated or formed a thin liquid layer, removing a significant amount of heat associated with the latent evaporator as well as convection effects. Some of the heat was also exchanged with the surrounding air, adding to the complication of this physical process. Although research in this area is very active, the mechanisms of heat transfer remain unknown. Because this study only concerned with very low heat flow and temperature, the heat loss due to spray generated between the water spray and the PV panel surface is calculated according to Eq. 19 [18].

$$q_{sp} = A_{PV} \times h_w \times (T_{PV} - T_w)$$
$$h_w = Nu_{sp} \times \frac{k_w}{L_{PV}}$$
$$\xi = \frac{T_{PV}}{T_{boiling} - T_{air}} \quad (19)$$
$$Nu_{sp} = 7.144 \times {Re_{sp}}^{0.438} \times \xi^{0.9016}$$
$$Re_{sp} = \frac{MF \times L_{PV}}{\mu_w} = \frac{MF_w \times \rho_w}{A_{pv}} \times \frac{L_{PV}}{\mu_w}$$

where h_w is the average heat transfer coefficient between the water spray and the PV panel

surface, W/m²/K; Nu_{sp} is the spray Nusselt number; k_w is the water thermal conductivity, W/m/K; L_{PV} is the PV panel length, m; T_{PV} is the temperature of the PV panel, °C; T_w is the water spray temperature, °C; A_{PV} is the surface area of the PV panels, m²; ζ is the non-dimensional temperature; T_{air} is the air temperature, °C; $T_{boiling}$ is the evaporating temperature of the water, °C; Re_{sp} is the spray Reynolds number; MF is the mass flux of water based on the unit area of the target PV panel surface, kg/m²/s; μ_w is the water's dynamic viscosity, Pa·s; MF_w is the mass flow rate, m³/s; ϱ_w is the water density, kg/m³.

In this study, a pump motor with a maximum flow of 12 litres per minute (equivalent to 0.0002 m³/s) was chosen, with the cooling water temperature assumed constant at 25 °C, water density of 997.1 kg/m³, water's dynamic viscosity of 0.0008905 Pa.s, and water thermal conductivity of 0.5948 W/m/K [3].

3.4 Photovoltaic panel electrical model

In practice, PV panel manufacturers usually provide three typical points of *I–V* curves and their heat coefficients. They are short-circuit current, open-circuit voltage, and maximum power (P_{MP_STC}) under standard test conditions (G_{STC} = 1000 W/m² and T_C = 25 °C), besides the corresponding thermal coefficients. To simplify the model, we calculated the maximum power of the PV panels according to Eq. 20 [6].

$$P_{MP}(G, T_C) = P_{MP\_STC} \times \frac{G}{G_{STC}} \times [1 + \alpha_P \times (T_{PV} - T_{STC})] \quad (20)$$

where P_{MP_STC} is the maximum power under standard test conditions, W; α_P is the thermal coefficient of power, %/°C. G is the total solar radiation shining on the surface area of solar cells of PV panels, W/m² and was calculated according to Eq. 21

$$G = G_t \times \tau_g \quad (21)$$

where τ_g is the transmissivity of the PV panel protection glass.

4 Results and discussion

The proposed simple thermal-electrical model was built and simulated with version 2015a of Matlab-Simulink software. The input data in this study are Solcast 2020 weather parameters, including *GHI*, *DNI*, *DHI*, air temperature, and wind speed. Hue City has two distinct hot, dry and wet, rainy seasons. The hot, dry season is from February to August, and the wet, rainy season is from September to January. We chose two typical weather cases for the research: a sunny day with few clouds in the hot, dry season (August 25) and a sunny day with clouds in the wet, rainy season (November 13). We compared the performance of the PV panels with four different systems: fixed-tilt panels with a tilt angle equal to latitude, fixed-tilt panels with a cooler, single-axis panels with a sun tracker, and cooler-integrated single-axis panels with a sun tracker (proposed system). These systems were labelled as follows: Normal, Cooler, Tracker, and Hybrid.

4.1 Sunny day with few clouds in hot, dry season

Fig. 3 illustrates weather data on the sunny day with few clouds in the hot, dry season. This is a typical summer day, with the highest air temperature of 35.7 °C at noon, lasting from 11 a.m. to 4 p.m., and the lowest wind speed. When the global horizontal irradiance reached 951 W/m², there were fewer clouds to reduce radiation. The total solar radiation for the day was 7.03 kWh/m².

The output power and temperature of the PV panels with different systems are shown in Fig. 4. It is clear that the power output of the PV panels with the single-axis sun tracker was highly

pISSN 1859-1388
eISSN 2615-9678

effective in the morning, from 6 a.m. to 11 a.m., and in the afternoon, from 1 p.m. to 5 p.m. compared with fixed-tilt systems. At noon, both systems had the same output power because they were equally inclined.

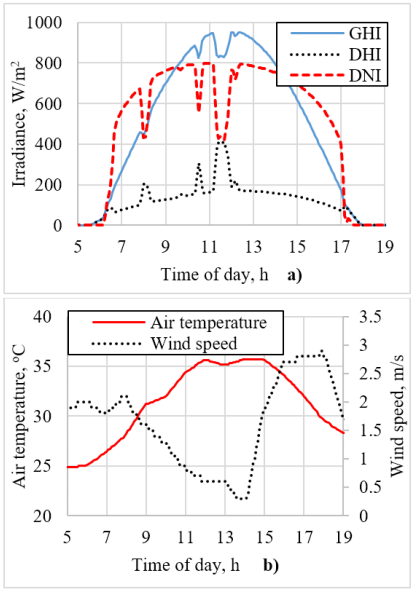

Fig. 3. Weather data on sunny day with few clouds in dry season, a) *GHI, DNI, DHI*; b) Air temperature and wind speed

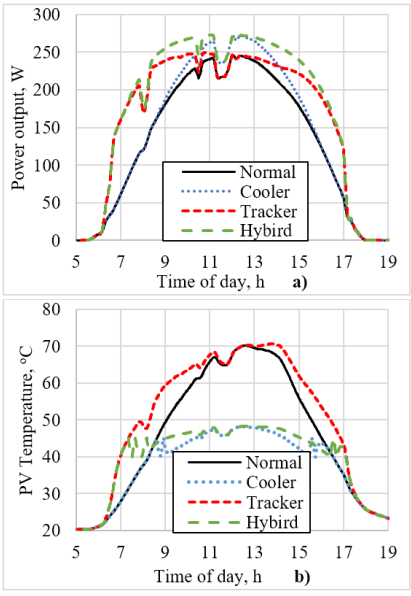

Fig. 4. Power output and temperature of PV panels using different systems in sunny day with few clouds in the dry season

The simulation results of the PV panels with the single-axis sun tracker are consistent with the experimental results reported previously [10]. In the case of the PV panels with a cooler, the temperature was lower, and the effect was improved compared with that of the fixed-tilt system between 9 a.m. and 3 p.m. The PV panels with a cooler-integrated sun tracker had these two advantages simultaneously, so their efficiency was higher than that of the fixed-tilt system during the working day. The power improvement efficiency of the PV panels with the proposed system increased to 32.76, 24.31, and 7.48% compared with the fixed-tilt system, the cooler, and the sun tracker. The obtained results can also be seen in experimental studies [12].

The temperature of the PV panels with the cooler and the proposed system at noon fluctuated between 40 and 48 °C. For the PV panels with the fixed-tilt system and the sun tracker, the temperature at noon was around 70 °C. The simulated PV panel temperature was higher than the actual value obtained in the experimental study [8]. This is due to higher air temperature and reduced wind speed at noon on the study day.

4.2 Sunny day with clouds in wet, rainy season

Fig. 5 depicts the weather data from the sunny day with clouds (November 13), typical of the wet, rainy season. The highest air temperature was 25.2 °C at noon, which lasted from 12 noon to 2 p.m., and the wind speed was at its highest value during the day. The global horizontal irradiance peaked at 541 W/m^2. Numerous cloudy periods during the day reduced the amount of direct normal irradiance to zero, and the total solar radiation was 2.99 kWh/m^2.

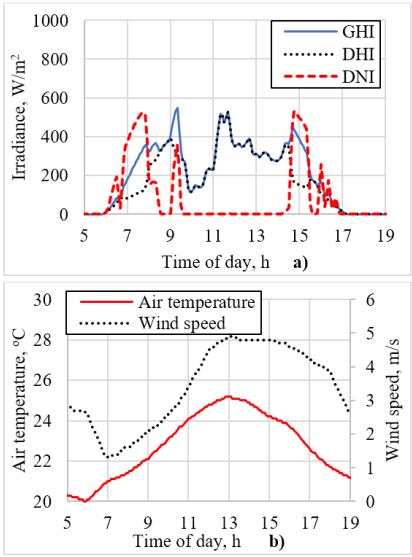

Fig. 5. Weather data of sunny day with clouds in wet, rainy season, a) *GHI*, *DNI*, *DHI*; b) Air temperature and wind speed

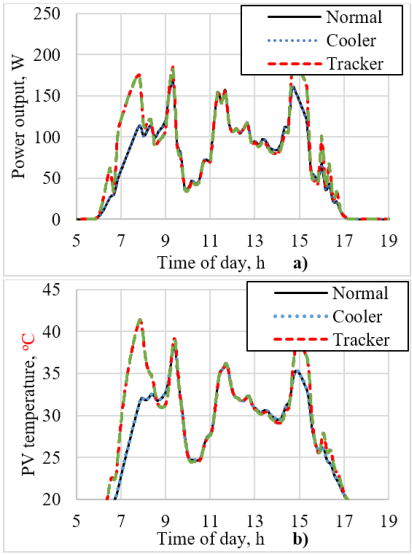

Fig. 6. Power output and temperature of PV panels with different systems in sunny day with clouds in the wet, rainy season

The output power and temperature of the PV panels with different systems are shown in Fig. 4. It is clear that the power output of the PV panels with the single-axis sun tracker was highly effective in the morning, from 6 a.m. to 11 a.m., and in the afternoon, from 1 p.m. to 5 p.m. compared with fixed-tilt systems. At noon, both systems had the same output power because they were equally inclined.

Fig. 6 depicts the power output and temperature of the PV panels with different systems. The low air temperature combined with the high wind caused the temperature of the PV panels not to exceed the cooler's set temperature (45 °C), so the cooler barely worked during the day, resulting in zero performance improvement in the PV panels with the cooling system. The total irradiance was low during the day, but the PV panel with the sun tracker and the proposed system provided a high efficiency, with a 12.55% improvement for the fixed-tilt PV panels.

4.3 Improved overall efficiency

Fig. 7 depicts the average daily *GHI* and air temperature. Obviously, during the dry-season months, the average daily *GHI* was relatively high, between 5.8 and 6.8 kWh/m², and the average temperature was also high, between 27.5 and 28.5 °C. In October, November, and December, the average daily *GHI* was low because of low air temperature.

The monthly energy output of the PV panels with the proposed system (Hybrid) compared with the other systems (Normal, Cooler, and Tracker) in one year is shown in Fig. 8. It is clear that the monthly energy output of the PV panels with the Hybrid is higher than that of the others, markedly in May, June, and July, which are hot, dry months. During the months of the wet, rainy season, the monthly energy output of the systems was not high because of low radiation and low average air temperature, so the efficiency was also down.

pISSN 1859-1388
eISSN 2615-9678

Table 3 shows the improved efficiency of the PV panels with the proposed system compared with the others. It is clear that the proposed system in the hot, dry season exhibited more improvement than in the wet, rainy season. During the hot, dry season, the PV panels with the proposed system gave the most significantly improved efficiency with 3.97, 13.61, and 17.27% compared with the PV panels with Tracker, Cooler, and Normal. In one year, the PV panels with the proposed system brought an improved overall efficiency of 16.35, 13.03, and 3.68% compared with the PV panels with the fixed-tilt system, cooler system, and sun tracker. The PV panels with the sun tracker were more beneficial than those with the cooler in one year.

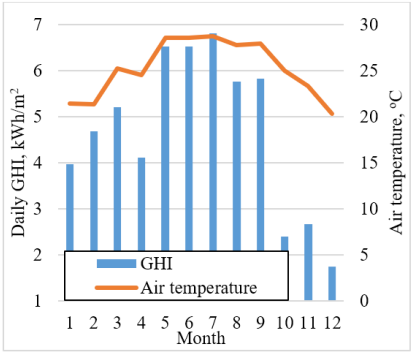

Fig. 7. Average daily *GHI* and average air temperature

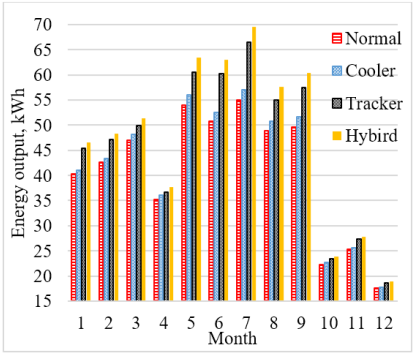

Fig. 8. Monthly energy output of PV panel with different systems

Table 3. Improved efficiency of PV panel using proposed system compared with other system

		Tracker	Cooler	Normal
Improved efficiency, %	In the hot dry season	3.97	13.61	17.27
	In the wet and rainy season	3.06	11.78	14.37
	overall	3.68	13.03	16.35

5 Conclusion

In this study, we built a simple thermal-electrical model of a PV panel with the cooler-integrated single-axis sun tracker. We also analyzed the overall efficiency of the photovoltaic panels and compared four systems: fixed tilt panels with a tilt angle equal to latitude, fixed tilt panels with a cooler, single-axis panels with a solar tracker, and the proposed system under different typical weathers within one year. On a sunny day with few clouds during the dry season, the efficiency of the PV panels with the proposed system increased to 32.76% compared with the fixed-tilt systems. On sunny days with clouds in the wet, rainy season, the PV panel temperature was lower than the cooler's initial set temperature, and the performance of the PV panels with the proposed system improved by 12.55% compared with the fixed-tilt system.

Over one year, the overall efficiency of the proposed system improved by 16.35, 13.03, and 3.68% compared with the PV panels with the fixed-tilt system, the cooler, and the single-axis sun tracker, respectively. These simulation results provide significant data for further research. Additionally, it is necessary to develop real models in different regions under other conditions, to better understand the improved efficiency of the PV panels with the proposed system.

DOI: 10.26459/hueunijns.v131i1D.6763

Funding statement

This research was funded by Hue University under grant No. DHH2021-18-01.

Nomenclature

albedo	Ground albedo
AOI	Angle of incidence, degree
A_{PV}	Surface area of PV panels, m^2
B	Variable for correction time, degree
C_p	Specific heat, kJ/kg/K
C_{PV}	Equivalent thermal capacitance of PV panel, J/K
DHI	Diffuse horizontal irradiance, W/m^2;
DNI	Direct normal irradiance, W/m^2;
E	Correction time, minute;
G	Total solar radiation shining on the surface area of solar cells of PV panels, W/m^2
G_b	Beam irradiance, W/m^2
G_d	Sky-diffuse irradiance, W/m^2
G_g	Ground-reflected irradiance, W/m^2
GHI	Global horizontal irradiance, W/m^2
G_t	Solar irradiance on PV panel surface, W/m^2
h_{conv}	convection heat transfer coefficient, $W/m^2/K$
h_w	Average heat transfer coefficient between water spray and PV panel surface, $W/m^2/K$
k_w	Water thermal conductivity, W/m/K
L_{loc}	Longitude of the studied area, degree
L_{PV}	PV panel length, m
LST	Local solar time, h
L_{stm}	Longitude of the standard meridian for the local time zone, degree
MF	Mass flux of water based on the unit area of the target PV panel surface, $kg/m^2/s$
MF_w	Mass flow rate, m^3/s;
n	Day number during a year
Nu_{sp}	Spray Nusselt number
P_{MP}	Electric power output of PV panel, W
P_{MP_STC}	Maximum power at standard test conditions, W.
q_{conv}	Convective heat transfer between the PV panel surface and the air, W
q_{rad_s}	Radiation heat transfer between the PV panel and the sky, W
q_{rad_g}	Radiation heat transfer between the PV panel and the ground, W
q_{ref}	Reflected solar irradiance, W
q_{sp}	Convective heat transfer between the PV panel and water spray, W
R	Rotation angle, degree
Re_{sp}	Spray Reynolds number
ST	Standard time, h
T_{air}	Air temperature, °C;
$T_{boiling}$	Evaporating temperature of water, °C
T_{PV}	Temperature of PV panel, °C
T_{sky}	Sky temperature, °C
T_w	Water spray temperature, °C
v_{wind}	Wind speed, m/s
x	Thickness, mm
α_P	Thermal coefficient of power, % /°C
γ_s	Solar azimuth, degree

pISSN 1859-1388
eISSN 2615-9678

δ	Solar declination, degree
ε_{rad}	Thermal emissivity of the PV panel
ζ	Non-dimensional temperature
θ_A	Azimuth angles of PV panel surface, degree
$\theta_{A,axis}$	Azimuth angle of the axis of rotation, degree
θ_T	Tilt angle of PV panel surface, degree
$\theta_{T,axis}$	Axis tilt angle, degree
θ_z	Solar zenith, degree
μ_w	Water dynamic viscosity, Pa.s
ϱ	Density of material, kg/m^3
ϱ_w	Water density, kg/m^3;
σ	Stephan-Boltzmann constant, W/m^2/K^4
τ_g	Transmissivity of PV panel protection glass
φ	Latitude of the studied area, degree
ω	Hour Angle, degree

References

1. Cuong NX, Hong NT, Tuan DA, Nhu YD. Performance Ratio Analysis Using Experimental Combining Historical Weather Data for Grid-Connected PV Systems. In: Sattler K, Nguyen DC, Vu NP, Long BT, Puta H, editors. Advances in Engineering Research and Application ICERA 2020 Lecture Notes in Networks and Systems. 178: Springer, Cham; 2021.
2. da Silva VO, Martinez-Bolanos JR, Heideier RB, Gimenes ALV, Udaeta MEM, Saidel MA. Theoretical and experimental research to development of water-film cooling system for commercial photovoltaic modules. IET Renewable Power Generation. 2021;15(1):206-24.
3. Dinçer İ, Zamfirescu C. Drying phenomena: theory and applications. West Sussex: John Wiley & Sons; 2016.
4. Goswami DY, Kreith F, Kreider JF. Principles of solar engineering: CRC Press; 2000.
5. Liang H, Han H, Wang F, Cheng Z, Lin B, Pan Y, et al. Experimental investigation on spectral splitting of photovoltaic/thermal hybrid system with two-axis sun tracking based on SiO_2/TiO_2 interference thin film. Energy Conversion Management. 2019;188:230-40.
6. Marion B, editor Comparison of predictive models for photovoltaic module performance. 2008 33rd IEEE Photovoltaic Specialists Conference; 2008: IEEE.
7. Marion WF, Dobos AP. Rotation angle for the optimum tracking of one-axis trackers. National Renewable Energy Lab.(NREL), Golden, CO (United States); 2013.
8. Mohanraj M, Chandramohan P, Sakthivel M, Kamaruzzaman S. Performance of photovoltaic water pumping systems under the influence of panel cooling. Renewable Energy Focus. 2019;31:31-44.
9. Mousavi Maleki SA, Hizam H, Gomes C. Estimation of hourly, daily and monthly global solar radiation on inclined surfaces: Models re-visited. Energies. 2017;10(1):134.
10. Ngo XC, Nguyen TH, Do NY, Nguyen DM, Vo D-VN, Lam SS, et al. Grid-connected photovoltaic systems with single-axis sun tracker: case study for Central Vietnam. Energies. 2020;13(6):1457.
11. Nižetić S, Čoko D, Yadav A, Grubišić-Čabo F. Water spray cooling technique applied on a photovoltaic panel: The performance response. Energy conversion management. 2016;108:287-96.
12. Ocłoń P, Cisek P, Kozak-Jagieła E, Taler J, Taler D, Skrzyniowska D, et al. Modeling and experimental validation and thermal performance assessment of a sun-tracked and cooled PVT system under low solar irradiation. Energy Conversion Management. 2020;222:113289.
13. Perovic B, Klimenta D, Jevtic M, Milovanovic M. A transient thermal model for flat-plate photovoltaic systems and its experimental validation. Elektronika ir Elektrotechnika. 2019;25(2):40-6.
14. Shahverdian MH, Sohani A, Sayyaadi H. Water-energy nexus performance investigation of water flow cooling as a clean way to enhance the productivity of solar photovoltaic modules. Journal of Cleaner Production. 2021;312:127641.
15. Sohani A, Shahverdian MH, Sayyaadi H, Hoseinzadeh S, Memon S. Enhancing the renewable energy payback period of a photovoltaic power generation system by water flow cooling.

International Journal of Solar Thermal Vacuum Engineering. 2021;3(1):73-85.

16. Solcast. Solar Irradiance Data [internet]. [updated 2021 November 20]. Available from: https://solcast.com.au.
17. Su Y, Zhang Y, Shu L. Experimental study of using phase change material cooling in a solar tracking concentrated photovoltaic-thermal system. Solar Energy. 2018;159:777-85.
18. Wang Y, Liu M, Liu D, Xu K, Chen Y. Experimental study on the effects of spray inclination on water spray cooling performance in non-boiling regime. Experimental Thermal Fluid Science. 2010;34(7): 933-42.